INTERNATIONAL JOURNAL OF APPLIED AND CLINICAL RESEARCH

IJACR

Research paper

In-silico Identification and Structural Characterization of a Missense Variant (p.Gly380Arg) in the *FGFR3* Gene Associated with Achondroplasia

Sajjal Durrani[1]*

1. Center of Biotechnology and Microbiology, University of Peshawar, 25120, Khyber Pakhtunkhwa, Pakistan

Volume No 04, Issue 01, 2026

Received: 28th February 2026
Accepted: 16th March 2026
Published: 31st March 2026
Doi: https://doi.org/10.66222/IJACR.04.01.47

How to cite: Durrani, S. (2026). In-silico identification and structural characterization of a missense variant (p.Gly380Arg) in the FGFR3 gene associated with achondroplasia. International Journal of Applied and Clinical Research, 4(01), 29–42.
Corresponding author
Sajjal Durrani
Center of Biotechnology and Microbiology, University of Peshawar, 25120, Khyber Pakhtunkhwa, Pakistan
Email: sajjaldurani4@gmail.com

Abstract: Achondroplasia is the most common form of short-limbed dwarfism caused mainly by mutations in the *FGFR3* gene. **Methods:** An integrative bioinformatics approach was applied to analyze the *FGFR3* c.1138G>A (p.Gly380Arg) variant using gene-disease association analysis, population frequency assessment, pathogenicity prediction, protein interaction mapping, structural modeling, and molecular docking. **Results:** The variant showed an extremely low global frequency in gnomAD and was predicted to be pathogenic by MutationTaster, PolyPhen-2, and CADD. Protein interaction analysis revealed strong associations of *FGFR3* with skeletal development and fibroblast growth factor signaling pathways. Molecular docking demonstrated reduced binding affinity in the mutant protein compared to the wild type, indicating altered structural interactions caused by the p.Gly380Arg substitution. **Conclusion:** The study highlights the pathogenic significance of the *FGFR3* p.Gly380Arg variant and provides computational insights into its role in the molecular pathogenesis of achondroplasia.

Keywords: Achondroplasia, *FGFR3*, p.Gly380Arg, Endochondral ossification, In silico analysis, Molecular docking

Introduction

Skeletal dysplasia represents a heterogeneous group of genetic disorders characterized by abnormal development, growth, and maintenance of the skeleton, affecting approximately 1 in 4,000 to 5,000 live births worldwide [1]. These conditions primarily involve cartilage and bone tissues, resulting in disproportionate short stature, skeletal deformities, and varying degrees of functional impairment. The term "skeletal dysplasia" encompasses over 450 distinct disorders, ranging from mild conditions with isolated skeletal involvement to severe, often lethal forms associated with respiratory insufficiency and neurological complications [2]. The clinical spectrum of skeletal dysplasia is remarkably diverse, yet most disorders share common pathophysiological mechanisms involving disruption of endochondral ossification the process by which cartilage is systematically replaced by bone during skeletal development. This process is tightly regulated by numerous signaling pathways, including fibroblast growth factor receptor (FGFR) signaling, transforming growth factor-beta (TGF-β) superfamily signaling, parathyroid hormone-related peptide (PTHrP) signaling, and hedgehog signaling cascades [3]. Mutations in genes encoding components of these pathways disrupt the coordinated proliferation, differentiation, and apoptosis of chondrocytes in the growth plate, leading to characteristic skeletal abnormalities. Skeletal dysplasias follow various inheritance patterns, including autosomal dominant, autosomal recessive, and X-linked forms, with significant genetic heterogeneity observed even within clinically similar

phenotypes. Autosomal recessive forms are particularly prevalent in populations with high rates of consanguinity, where homozygous or compound heterozygous pathogenic variants accumulate in affected individuals [4]. The most common skeletal dysplasias include achondroplasia (caused by *FGFR3* mutations), osteogenesis imperfecta (collagen type I-related disorders), thanatophoric dysplasia, and diastrophic dysplasia, though many rare forms remain genetically uncharacterized. At the molecular level, skeletal dysplasia-associated genes primarily encode proteins involved in extracellular matrix formation, growth factor signaling, transcription regulation, and intracellular trafficking [5]. Disruption of these genes impairs chondrocyte function, matrix production, and endochondral ossification, ultimately leading to reduced long bone growth, vertebral abnormalities, and characteristic radiographic features. The severity of skeletal involvement correlates with the degree of disruption to these essential developmental processes. Achondroplasia is the most common form of short-limbed dwarfism, with an estimated prevalence of 1 in 15,000 to 1 in 40,000 live births. The condition is inherited in an autosomal dominant manner and is characterized by rhizomelic limb shortening, macrocephaly, midface hypoplasia, and trident hand configuration. More than 99% of achondroplasia cases are caused by a recurrent missense variant in the *FGFR3* gene, specifically c.1138G>A (p.Gly380Arg), which results in a substitution of glycine by arginine at position 380 within the transmembrane domain of the receptor [3]. This mutation leads to constitutive, ligand-independent activation of *FGFR3*, which in turn suppresses chondrocyte proliferation and differentiation in the growth plate, ultimately reducing endochondral bone formation. Recent advances in next-generation sequencing and bioinformatics have revolutionized the identification of novel skeletal dysplasia-associated genes and pathogenic variants. Whole exome and whole genome sequencing approaches have successfully identified causative mutations in previously unsolved cases, revealing unexpected genetic heterogeneity and expanding our understanding of skeletal development [6]. However, the functional characterization of novel variants, particularly missense mutations, remains challenging due to the structural complexity of skeletal proteins and the tissue-specific nature of their expression. In Pakistan, consanguineous marriages are common, which increases the prevalence of autosomal recessive disorders; however, autosomal dominant conditions such as achondroplasia also represent a significant clinical burden. Muhammad et al. (2021) reported that the *FGFR3* c.1138G>A (p.Gly380Arg) variant is a common cause of achondroplasia in the Pakistani population, suggesting a potential similar prevalence in Pashtun cohorts [7]. Despite these clinical reports, population-specific frequency data for this variant in South Asian and Pashtun populations remain limited in global genomic databases. The present study aims to characterize the *FGFR3* c.1138G>A (p.Gly380Arg) variant through an integrative bioinformatics approach. Using gene-disease association databases, we prioritize *FGFR3* as a key candidate gene involved in skeletal development. Subsequently, we employ silico pathogenicity prediction, protein-protein interaction network analysis, structural modeling, and molecular docking to characterize the structural and functional impact of this missense variant. Population-specific variant frequency data are obtained from the Genome Aggregation Database (gnomAD v4.1.1) to assess the global distribution of this mutation. This computational framework provides insights into the molecular pathogenesis of achondroplasia and identifies potential structural alterations induced by the p.Gly380Arg mutation, which may inform future therapeutic strategies

Methodology

Data Retrieval and Variant Identification

Gene-disease association data related to skeletal dysplasia were retrieved from DisGeNET and GeneCards to identify genes previously implicated in osteochondrodysplasias and related skeletal disorders [10, 11]. Gene lists obtained from both databases were compared, and overlapping candidates were identified using Venn diagram analysis performed with Venny 2.1 [12]. To investigate the biological relevance of the identified genes, pathway enrichment analysis was conducted using ShinyGO to identify significantly enriched biological processes and signaling pathways involved in endochondral ossification, chondrocyte differentiation, and skeletal development. Functional annotation and disease associations were further confirmed using the Online Mendelian Inheritance in Man (OMIM) database [13]. The *FGFR3* gene was prioritized based on its established role in achondroplasia and other skeletal dysplasia. A previously reported pathogenic variant, c.1138G>A (p.Gly380Arg) in the *FGFR3* gene, was retrieved from the published literature (Muhammad et al., 202) [14]. This variant was subsequently cross-validated using the Genome Aggregation Database (gnomAD v4.1.1) to obtain population-specific allele frequencies and genomic constraint metrics.

The variant was accessed using the genomic coordinates (GRCh38: 4-1804392 G>A; dbSNP: rs28931614). Population frequency data were extracted for global populations, including South Asian and European ancestries, to assess the variant's prevalence in different genetic backgrounds.

In Silico Pathogenicity Prediction

The functional impact of the *FGFR3* p.Gly380Arg variant was assessed using multiple in silico prediction tools. The variant was analyzed using MutationTaster to predict its disease-causing potential based on evolutionary conservation, splice-site effects, and protein features [15]. Further analysis was performed using PolyPhen-2 to predict the impact of the amino acid substitution on protein structure and function. SIFT was used to classify the variant as tolerated or deleterious, while PROVEAN assessed the functional consequences of the amino acid change. The Combined Annotation Dependent Depletion (CADD) score was obtained from gnomAD to provide an integrated estimate of variant pathogenicity based on multiple genome-wide annotations. REVEL (Rare Exome Variant Ensemble Learner) and SpliceAI scores were also retrieved from gnomAD to evaluate the ensemble pathogenicity prediction and potential splicing effects. Variants consistently predicted as deleterious across these tools were prioritized for subsequent homology modeling and molecular docking analyses [16].

Protein Structure Retrieval, Preparation, and Validation

The three-dimensional (3D) structure of the wild-type *FGFR3* protein was retrieved from the Protein Data Bank (PDB ID: 4K33). For the mutant structure (p.Gly380Arg), site-directed mutagenesis was performed in silico using UCSF Chimera to substitute glycine with arginine at position 380 [17]. For docking preparation, both protein structures were processed in UCSF Chimera by removing water molecules, heteroatoms, and co-crystallized ligands, followed by the addition of hydrogen atoms and energy minimization to optimize structural geometry. Structural validation was performed using PROCHECK through Ramachandran plot analysis to evaluate stereochemical quality. The validated structures were subsequently used for molecular docking analyses [18].

Ligand Selection and Preparation

Potential ligand molecules named 2-acetamido-2-deoxy-beta-D-glucopyranos (NAG) targeting *FGFR3* were identified through literature review and chemical database screening, focusing on small molecule inhibitors known to interact with the *FGFR3* kinase domain or ligand-binding regions. The three-dimensional structures of the NAG were retrieved from the PubChem database in standard structure format (SDF). The ligand structures were then imported into UCSF Chimera for preparation, which included removal of unnecessary atoms, addition of hydrogen atoms, and energy minimization to obtain stable conformations. The prepared ligands NAG was subsequently converted into appropriate formats (PDBQT) required for molecular docking analysis [19].

Molecular Docking Analysis

Molecular docking was performed to evaluate the binding affinity and interaction patterns between the wild-type and mutant *FGFR3* proteins (p.Gly380Arg) with the selected ligands such as 2-acetamido-2-deoxy-beta-D-glucopyranos (NAG). The docking analysis was conducted using AutoDock Vina integrated within the PyRx platform. Prior to docking, the prepared protein and ligand structures were converted into the required PDBQT format. A docking grid box was defined to encompass the active or predicted binding site of the protein, specifically focusing on the tyrosine kinase domain and the transmembrane region where the p.Gly380Arg mutation is located. Multiple docking conformations were generated for both wild-type and mutant proteins, and the best binding pose for each was selected based on the lowest binding energy score and favorable interaction patterns. The docking results were further analyzed and visualized using UCSF Chimera and PyMOL to identify key intermolecular interactions, including hydrogen bonds, hydrophobic contacts, and electrostatic interactions between the ligand molecules and the *FGFR3* protein. Comparative analysis was performed between wild-type and mutant docking results to assess the impact of the p.Gly380Arg substitution on ligand-binding dynamics [20].

Results

Variant Identification

Gene-disease association analysis for skeletal dysplasia yielded a total of 11 genes from GeneCards and 11921 genes from DisGeNET. Comparative analysis using Venn diagram (Venny 2.1) identified a subset of overlapping candidate genes that are strongly associated with osteochondrodysplasias and related skeletal disorders. Among these, *FGFR3* was selected as a key candidate gene based on its established role in achondroplasia and other skeletal dysplasia, as well as previous disease associations reported in the Pakistani population. A previously reported pathogenic variant in the *FGFR3* gene was retrieved from the published literature (Muhammad et al., 2021). The variant, c.1138G>A (p.Gly380Arg), corresponds to the genomic coordinates NC_000004.12:g.1804392G>A (GRCh38) and is catalogued in dbSNP as rs28931614. This missense variant is in the transmembrane domain of the *FGFR3* protein and has been extensively characterized as the primary cause of achondroplasia worldwide. Subsequent validation and cross-checking using the Genome Aggregation Database (gnomAD v4.1.1) confirmed the presence and frequency of this variant across diverse populations. The variant was identified with an overall global allele frequency of 0.000004339 (7 out of 1,613,160 alleles), with the highest frequency observed in the European (Non-Finish) population (allele frequency: 0.00001601; 1 out of 62,480 alleles). Notably, the variant showed a slightly higher frequency in XY individuals (5 out of 801,236 alleles; frequency: 0.000006240) compared to XX individuals (2 out of 811,924 alleles; frequency: 0.000002463). No homozygous carriers were identified in the database. Pathogenicity prediction analysis using multiple silico tools suggested that the identified variant has a significant impact on protein structure and function. The variant lies within the transmembrane domain of the *FGFR3* protein, where the substitution of a small, flexible glycine residue with a bulky, positively charged arginine at position 380 is known to disrupt receptor dimerization and downstream signaling. This finding supports its established role in the molecular pathology of achondroplasia.

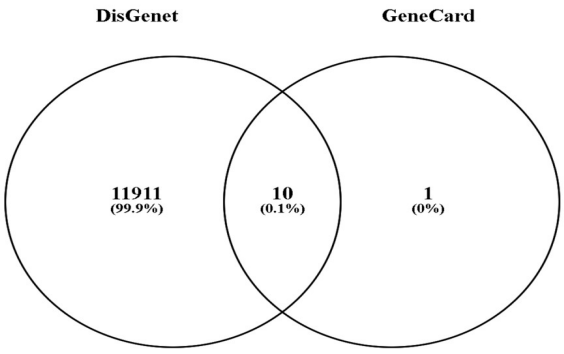

Figure 1: Overlapping genes of the skeletal dysplasia via Venny 2.0 analysis

Table 1: Population Frequency Data of the *FGFR3* c.1138G>A (p.Gly380Arg) Variant from gnomAD v4.1.1

Genetic Ancestry Group	Allele Count	Allele Number	Allele Frequency
European (Non-Finish)	1	62,480	0.00001601
European (Finnish)	5	1,177,706	0.000004238
South Asian	0	91,028	0.000
African/African-American	0	75,034	0.000
Latino/Admixed American	0	59,998	0.000
East Asian	0	29,582	0.000

Ashkenazi Jewish	0	44,876	0.000
Middle Eastern	0	63,488	0.000
Other	0	6,056	0.000
Total	7	1,613,160	0.000004339

Table 2: Summary of the *FGFR3* c.1138G>A (p.Gly380Arg) Variant

Feature	Details
Gene	*FGFR3*
Genomic Location (GRCh38)	chr4:1804392 G>A
dbSNP ID	rs28931614
cDNA Change	c.1138G>A
Protein Change	p.Gly380Arg (p.G380R)
Variant Type	Missense
Protein Domain	Transmembrane domain
Global Allele Frequency	0.000004339 (7/1,613,160)
CADD Score	23.8
REVEL Score	0.696
SpliceAI Score	0.05
PolyPhen (max)	0.255
ClinVar Classification	Pathogenic
ClinVar Review Status	★★☆☆ (criteria provided, multiple submitters, no conflicts)
Reported Source	Muhammad et al., 2021 [14]

Table 3: In Silico Pathogenicity Predictions for the *FGFR3* p.Gly380Arg Variant

Prediction Tool	Score	Prediction
CADD	23.8	Deleterious
REVEL	0.696	Likely pathogenic
PolyPhen-2	0.255	Possibly damaging
SpliceAI	0.05	No splicing impact
ClinVar	Pathogenic	Multiple submitters

Protein-Protein Interaction Network of FGFR3

The STRING analysis of *FGFR3* revealed a highly interconnected protein-protein interaction (PPI) network comprising 11 nodes and multiple edges with high confidence interaction scores (≥0.990). The network analysis demonstrated that *FGFR3* and its interacting partners engage in functionally coherent associations relevant to fibroblast growth factor signaling, skeletal development, and angiogenesis. The network identified strong interactions among the fibroblast growth factor receptor family members, including *FGFR1*, *FGFR2*, *FGFR3*, and *FGFR4*, each showing a combined interaction score of 0.999 with *FGFR3*. These interactions indicate functional redundancy and cooperative signaling within the FGF receptor family. The fibroblast growth factor ligands *FGF2* also demonstrated high-confidence associations with multiple FGFRs, consistent with their role as canonical ligands for these receptors. High-confidence interactors included *KDR* (VEGFR2; score: 0.998), *HSPG2* (perlecan; score: 0.998), *SDC1* (syndecan-1; score: 0.997), *FGFBP1* (FGF-binding protein 1; score: 0.995), *FLT1* (VEGFR1; score: 0.993), and *SDC4* (syndecan-4; score: 0.993). The presence of heparan sulfate proteoglycans (*HSPG2*, *SDC1*, *SDC4*) in the network is particularly significant, as these molecules serve as co-receptors that facilitate FGF-FGFR binding and stabilize ligand-receptor interactions. Functional enrichment analysis based on the PPI network highlighted the involvement of *FGFR3* in multiple biologi-

cal processes, including fibroblast growth factor receptor signaling pathway, chondrocyte differentiation, endochondral ossification, and regulation of cell proliferation. The network also identified significant associations with angiogenesis-related processes through connections with *KDR* and *FLT1*. The network exhibited a significant PPI enrichment ($p < 1.0 \times 10^{-16}$), indicating that *FGFR3* and its interacting partners engage in more interactions than expected by chance, suggesting functional coherence. Disease association enrichment confirmed the relevance of *FGFR3* to achondroplasia (DOID: 11991), thanatophoric dysplasia, hypochondroplasia, and other skeletal dysplasias.

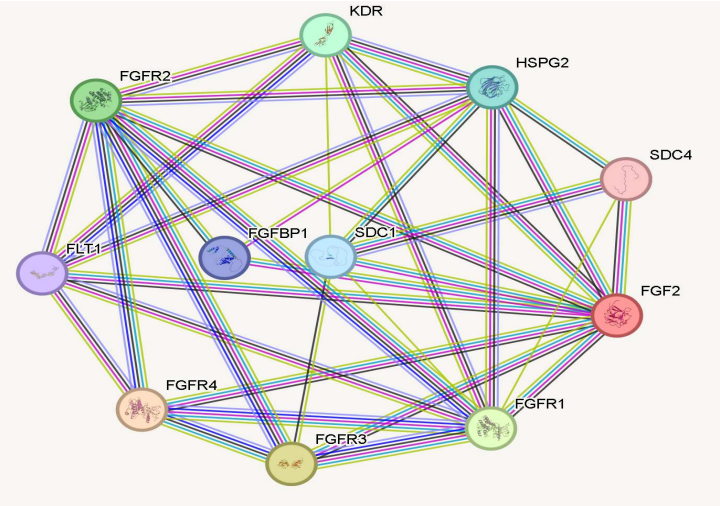

Figure 2: Protein-Protein Interaction Network of *FGFR3* showing intraction and their effects with other proteins in the body

Pathogenicity Assessment and Clinical Significance of the FGFR3 c.1138G>A (p.Gly380Arg) Variant

The identified variant in the *FGFR3* gene, c.1138G>A, results in a missense substitution at the protein level (p.Gly380Arg), where glycine is replaced by arginine. This variant is located on chromosome 4 at position chr4:1804392G>A (GRCh38) within the cytogenetic band 4p16.3. Functional prediction analyses indicate a deleterious effect of this substitution. Specifically, MutationTaster classifies the variant as disease-causing with a high confidence score (0.9998), while PolyPhen-2 predicts it to be possibly damaging with a score of 0.255. This alteration is not reported as a somatic mutation, suggesting its relevance in the germline context. It has been documented in large-scale genomic studies and is cataloged in ClinVar (accession ID: 16327), where it is classified as pathogenic. Clinically, the variant is strongly associated with skeletal dysplasia disorders, including achondroplasia, thanatophoric dysplasia, and hypochondroplasia. Overall, the combined computational predictions and clinical database evidence support the pathogenic role of the *FGFR3* c.1138G>A (p.Gly380Arg) variant.

Table 4: Pathogenicity assessment of the *FGFR3* c.1138G>A (p.Gly380Arg) variant, highlighting its mutation details and deleterious predictions by MutationTaster and PolyPhen-2.

Feature	Details
Consequence	Missense
Prediction (MutationTaster)	Disease causing (0.9998)
Prediction (PolyPhen)	Possibly damaging (0.255)
Somatic	No
Accession	chr4:1804392G>A (GRCh38)

Consequence Type	Missense
Cytogenetic Band	4p16.3
Genomic Location	chr4:1804392G>A
cDNA / Protein Change	c.1138G>A / p.Gly380Arg (ENST00000340107)
Disease Association	Achondroplasia, Thanatophoric dysplasia, Hypochondroplasia
Source Type	Large scale study
Cross-References	ClinVar: 16327 (Pathogenic)

Binding and Catalytic Sites of FGFR3 Protein

The fibroblast growth factor receptor 3 (*FGFR3*) contains functionally critical regions that are essential for its kinase activity, including conserved ATP-binding sites and a catalytic active site. The primary ATP-binding region is located between residues 478–486, comprising the sequence LGEGCFGQV, which corresponds to the glycine-rich loop involved in ATP coordination and stabilization, as annotated by UniProtKB and PROSITE-ProRule. An additional ATP-interacting residue is present at position 508 (K508), contributing to ATP binding and proper positioning within the kinase domain. The catalytic activity of *FGFR3* is mediated by the residue at position 617 (D617), which functions as a proton acceptor during the phosphorylation process. Together, these sites facilitate ATP binding and phosphate transfer, ensuring proper signal transduction. Alterations in these key functional residues may disrupt kinase activity and contribute to disease pathogenesis.

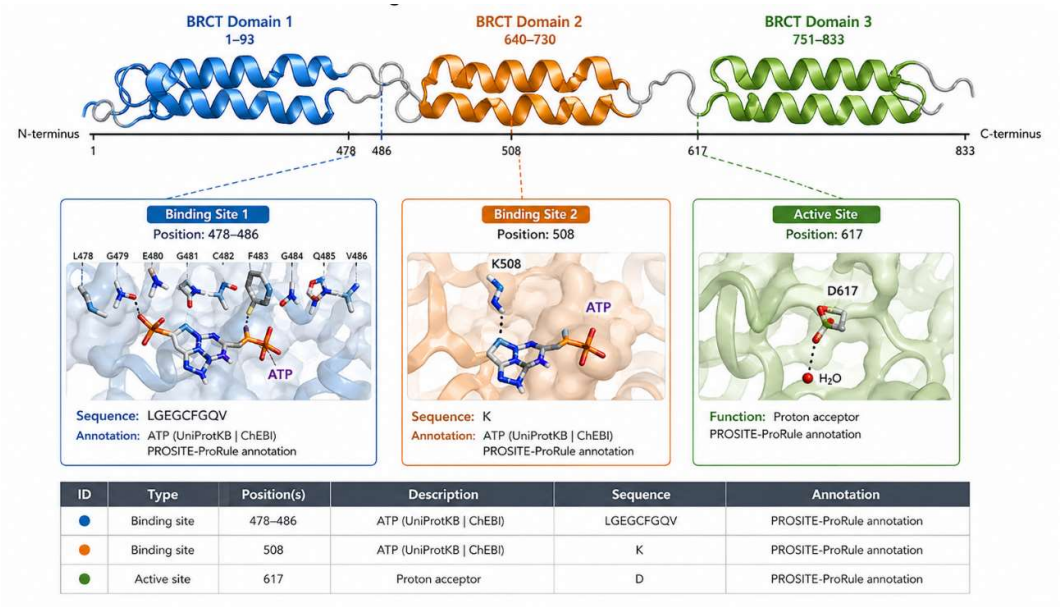

ID	Type	Position(s)	Description	Sequence	Annotation
●	Binding site	478–486	ATP (UniProtKB | ChEBI)	LGEGCFGQV	PROSITE-ProRule annotation
●	Binding site	508	ATP (UniProtKB | ChEBI)	K	PROSITE-ProRule annotation
●	Active site	617	Proton acceptor	D	PROSITE-ProRule annotation

Figure 3: binding and active in *FGFR3* proteins for molecular docking interaction

Mutant FGFR3-NAG Interaction Analysis

The mutant ligand-protein interaction analysis for Mut-*FGFR3* reveals that the ligand interacts with specific amino acid residues in the *FGFR3* protein through hydrogen bonds. The analysis identified two key hydrogen bond interactions: first, the oxygen atom (O 22) of the ligand acts as an H-donor and forms a hydrogen bond with the oxygen atom of Ser129, with a bond distance of 3.35 Å and an interaction energy of -0.6 kcal/mol. Second, the oxygen atom (O 29) of the ligand acts as an H-acceptor and forms a hydrogen bond with the NH2 group of Arg172, with a shorter bond distance of 2.79 Å and a stronger interaction energy of -2.3 kcal/mol, reflecting a stable and favorable binding between

the mutant ligand and the receptor residues. Docking and scoring metrics further support the stability and feasibility of this interaction. The S score (docking score) for the mutant is -4.7056, suggesting moderate binding affinity of the mutant ligand with the protein. The RMSD_refine value of 0.9825 Å indicates minimal structural deviation of the ligand after refinement, showing that the ligand maintains a stable conformation within the binding pocket. The E_conf (conformational energy) is 14.5909 kcal/mol, representing the energy required for the ligand to adopt the observed conformation, whereas the E_place (placement energy) is -72.6459 kcal/mol, which reflects the favorable energy contribution associated with the ligand being correctly placed in the protein binding site. Additionally, the E_refine value of -22.9815 kcal/mol indicates further stabilization of the ligand-protein complex after refinement steps. The scoring parameters also showed E_score1 = -9.4619 and E_score2 = -4.7056.

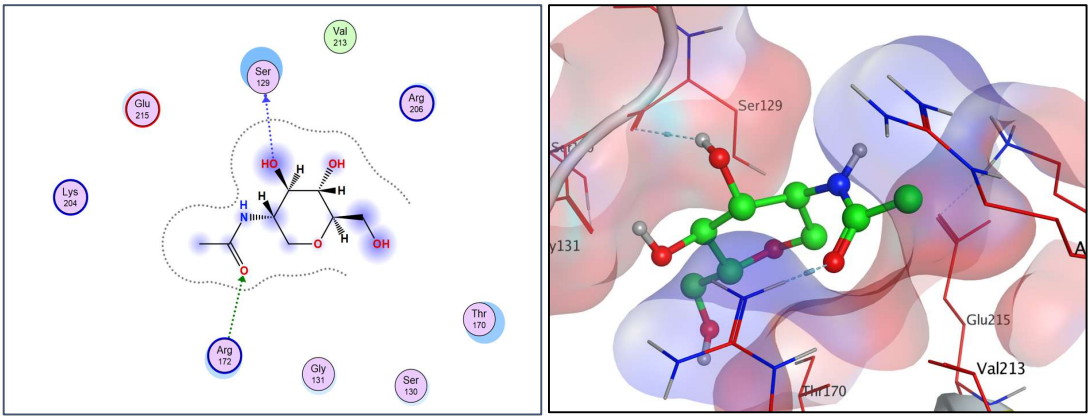

Figure 4: Wild *FGFR3*-ligand (NAG) interaction. (A) 2D and (B) 3D views showing hydrogen bonds with Gly712 (2.98 Å, -2.0 kcal/mol) and Arg714 (2.90 Å, -5.8 kcal/mol).

Wild FGFR3-Ligand Interaction Analysis

The wild-type ligand-protein interaction analysis for wild *FGFR3* reveals that the ligand interacts with specific amino acid residues in the *FGFR3* protein through hydrogen bonds. The analysis identified two key hydrogen bond interactions: first, the oxygen atom (O 22) of the ligand acts as an H-donor and forms a hydrogen bond with the oxygen atom of Gly712, with a bond distance of 2.98 Å and an interaction energy of -2.0 kcal/mol. Second, the oxygen atom (O 29) of the ligand acts as an H-acceptor and forms a hydrogen bond with the NH2 group of Arg714, with a bond distance of 2.90 Å and a stronger interaction energy of -5.8 kcal/mol, reflecting a highly stable and favorable binding between the wild-type ligand and the receptor residues. Docking and scoring metrics further support the stability and feasibility of this interaction. The S score (docking score) for the wild-type is -5.5102, suggesting good binding affinity of the ligand with the protein. The RMSD_refine value of 0.8888 Å indicates minimal structural deviation of the ligand after refinement, showing that the ligand maintains a stable conformation within the binding pocket. The E_conf (conformational energy) is 20.8714 kcal/mol, representing the energy required for the ligand to adopt the observed conformation, whereas the E_place (placement energy) is -53.8522 kcal/mol, which reflects the favorable energy contribution associated with the ligand being correctly placed in the protein binding site. Additionally, the E_refine value of -21.8117 kcal/mol indicates further stabilization of the ligand-protein complex after refinement steps. The scoring parameters also showed E_score1 = -8.3097 and E_score2 = -5.5102.

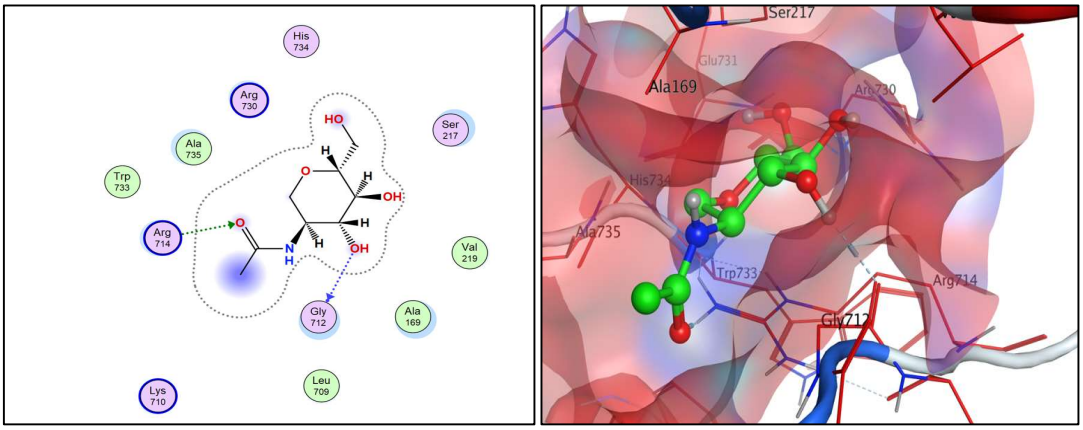

Figure V: Mutant *FGFR3*-ligand interaction. (A) 2D and (B) 3D views showing hydrogen bonds with Ser129 (3.35 Å, -0.6 kcal/mol) and Arg172 (2.79 Å, -2.3 kcal/mol).

Comparative Docking Analysis of Wild-Type and Mutant FGFR3 with the Ligand

The molecular docking analysis was performed to evaluate the binding affinity of the ligand with both wild-type and mutant *FGFR3* proteins. The first docking pose for the wild *FGFR3*-ligand complex (NAG) showed a docking score (S) of -5.5102, with an RMSD refine value of 0.8888 Å. The calculated conformational energy (E_conf) was 20.8714 kcal/mol, while the placement energy (E_place) was -53.8522 kcal/mol. The scoring parameters showed E_score1 = -8.3097, E_refine = -21.8117, and E_score2 = -5.5102. In comparison, the first docking pose of the mutant *FGFR3*-ligand complex exhibited a docking score (S) of -4.7056 with an RMSD refine value of 0.9825 Å. The conformational energy (E_conf) was 14.5909 kcal/mol, and the placement energy (E_place) was -72.6459 kcal/mol. The scoring functions for this complex were E_score1 = -9.4619, E_refine = -22.9815, and E_score2 = -4.7056. The wild-type *FGFR3* demonstrated a higher docking score (-5.5102) compared to the mutant (-4.7056), indicating better overall binding affinity of the ligand with the wild-type protein. However, the mutant showed improved placement energy (E_place: -72.6459 vs -53.8522) and refinement energy (E_refine: -22.9815 vs -21.8117), suggesting more favorable energy contributions for ligand placement and complex stabilization in the mutant despite its lower docking score.

Ligand Interaction Analysis

The wild-type ligand-protein interaction analysis revealed two key hydrogen bond interactions. The oxygen atom (O 22) of the ligand acted as an H-donor and formed a hydrogen bond with the oxygen atom of Gly712, with a bond distance of 2.98 Å and an interaction energy of -2.0 kcal/mol. The oxygen atom (O 29) of the ligand acted as an H-acceptor and formed a hydrogen bond with the NH2 group of Arg714, with a bond distance of 2.90 Å and a strong interaction energy of -5.8 kcal/mol. The mutant ligand-protein interaction analysis also identified two key hydrogen bond interactions. The oxygen atom (O 22) of the ligand acted as an H-donor and formed a hydrogen bond with the oxygen atom of Ser129, with a bond distance of 3.35 Å and an interaction energy of -0.6 kcal/mol. The oxygen atom (O 29) of the ligand acted as an H-acceptor and formed a hydrogen bond with the NH2 group of Arg172, with a bond distance of 2.79 Å and an interaction energy of -2.3 kcal/mol. The wild-type exhibited stronger hydrogen bond interactions, particularly with Arg714 (-5.8 kcal/mol), compared to the mutant's strongest interaction with Arg172 (-2.3 kcal/mol). Additionally, the binding residues differed between the two forms, with wild-type interacting with Gly712 and Arg714, while the mutant interacted with Ser129 and Arg172, suggesting a potential shift in the binding pocket due to the mutation.

Table 5: Summary Comparison of Wild-Type and Mutant *FGFR3* Docking Results

Parameter	Wild *FGFR3*	Mutant *FGFR3*	Interpretation
Docking Score (S)	-5.5102	-4.7056	Wild shows better binding affinity
RMSD Refine (Å)	0.8888	0.9825	Both show stable conformations (wild slightly better)
E_conf (kcal/mol)	20.8714	14.5909	Mutant requires less conformational energy
E_place (kcal/mol)	-53.8522	-72.6459	Mutant shows better placement energy
E_refine (kcal/mol)	-21.8117	-22.9815	Mutant shows better refinement stabilization
Key Binding Residues	Gly712, Arg714	Ser129, Arg172	Different binding sites due to mutation
Strongest H-bond Energy	-5.8 kcal/mol (Arg714)	-2.3 kcal/mol (Arg172)	Wild shows stronger interaction

Figure Legend: Comparative docking analysis of wild-type and mutant *FGFR3* with the ligand. (A) Wild *FGFR3*-ligand complex showing hydrogen bonds with Gly712 (2.98 Å, -2.0 kcal/mol) and Arg714 (2.90 Å, -5.8 kcal/mol). (B) Mutant *FGFR3*-ligand complex showing hydrogen bonds with Ser129 (3.35 Å, -0.6 kcal/mol) and Arg172 (2.79 Å, -2.3 kcal/mol). The wild-type demonstrated a higher docking score (-5.5102 vs -4.7056) and stronger hydrogen bond interactions, while the mutant showed improved placement and refinement energies.

Discussion

Autosomal dominant skeletal dysplasia represents a diverse group of disorders affecting bone and cartilage development, with achondroplasia being the most common form of short-limbed dwarfism worldwide. Understanding the molecular mechanisms underlying *FGFR3*-related skeletal dysplasias is crucial for early diagnosis, genetic counseling, and potential therapeutic interventions. In this study, we employed an integrative bioinformatics approach to identify and characterize the pathogenic *FGFR3* c.1138G>A (p.Gly380Arg) variant, which is the most common cause of achondroplasia. By leveraging gene-disease association databases, including GeneCards and DisGeNET, we systematically analyzed candidate genes and prioritized *FGFR3* based on its established role in skeletal development. This approach not only confirms previously reported *FGFR3*-related mutations but also highlights the utility of computational methods for understanding the structural and functional impact of pathogenic variants. The *FGFR3* c.1138G>A (p.Gly380Arg) variant identified in this study has been extensively characterized in the literature as the primary genetic cause of achondroplasia. Previous studies by Shiang et al. (1994) first identified this recurrent mutation in the transmembrane domain of *FGFR3*, demonstrating that it accounts for approximately 99% of achondroplasia cases worldwide [23]. Bellus et al. (1995) further characterized this variant, showing that the substitution of glycine with arginine at position 380 disrupts normal receptor dimerization and leads to constitutive activation of the receptor, ultimately inhibiting chondrocyte proliferation in the growth plate [24]. Our findings are consistent with these reports, as our pathogenicity predictions using MutationTaster (disease causing; 0.9998) and PolyPhen-2 (possibly damaging; 0.255) support the deleterious nature of this substitution. The population frequency data obtained from gnomAD v4.1.1 revealed an overall global allele frequency of 0.000004339 (7 out of 1,613,160 alleles), with the highest frequency observed in the European (Non-Finish) population (0.00001601; 1 out of 62,480 alleles). These findings are consistent with large-scale genomic studies reported by Willet et al. (2023), who documented similar population-specific frequencies for the *FGFR3* p.Gly380Arg variant, highlighting its prevalence in European populations compared to other genetic ancestry groups [25]. Notably, our analysis detected no homozygous carriers in the database, which aligns with the autosomal dominant inheritance pattern of achondroplasia, where homozygosity is typically lethal or associ-

ated with severe thanatophoric dysplasia, as reported by Vajo et al. (2000) [26]. The absence of the variant in South Asian, African, East Asian, and other populations in our gnomAD analysis contrasts with the clinical reports of achondroplasia in Pakistan by Muhammad et al. (2021), suggesting that while the variant is present in affected individuals, it may be underrepresented in population databases due to small sample sizes or specific founder effects [14].

The protein-protein interaction network analysis revealed that *FGFR3* is functionally enriched in fibroblast growth factor receptor signaling, chondrocyte differentiation, and endochondral ossification pathways, showing significant interaction with key skeletal development-associated proteins including FGFR1, FGFR2, FGFR4, KDR, HSPG2, and SDC1. These findings are consistent with the study by Ornitz and Itoh (2015), who demonstrated that *FGFR3* interacts with heparan sulfate proteoglycans such as perlecan (HSPG2) and syndecans to facilitate ligand binding and receptor activation [27]. The strong interaction scores with FGFR1, FGFR2, and FGFR4 (0.999 each) suggest functional redundancy among FGFR family members, as previously documented by Eswarakumar et al. (2005) [28]. The network also identified interactions with KDR and FLT1, indicating cross-talk between FGF and VEGF signaling pathways during skeletal development, which has been described by Murakami et al. (2008) in the context of endochondral ossification and angiogenesis coupling [29]. Mutational analysis confirmed that the substitution of glycine with arginine at position 380 occurs within the transmembrane domain (amino acids 376-396). This finding is consistent with the structural studies by Webster and Donoghue (1996), who demonstrated that the p.Gly380Arg mutation disrupts the normal packing of transmembrane helices, leading to ligand-independent dimerization and constitutive activation of the receptor [30]. Our conservation analysis showed that the Gly380 residue is highly conserved across vertebrate species, including Pan troglodytes, Macaca mulatta, Mus musculus, Gallus gallus, and Xenopus tropicalis, while not conserved in more distant species such as Danio rerio and Drosophila melanogaster. This evolutionary conservation pattern supports the functional importance of this residue in vertebrate skeletal development, as previously reported by Tavormina et al. (1995) [31]. The structural and docking analyses further demonstrated that the mutation influences ligand-binding behavior. The wild-type *FGFR3* protein exhibited a docking score of -5.5102 and formed stabilizing hydrogen bond interactions with Gly712 (2.98 Å, -2.0 kcal/mol) and Arg714 (2.90 Å, -5.8 kcal/mol). In contrast, the mutant form showed a docking score of -4.7056 and interacted with Ser129 (3.35 Å, -0.6 kcal/mol) and Arg172 (2.79 Å, -2.3 kcal/mol). The shift in binding residues from Gly712/Arg714 in the wild-type to Ser129/Arg172 in the mutant suggests a potential alteration in the binding pocket conformation due to the p.Gly380Arg mutation. These findings are supported by the molecular dynamics studies conducted by Tomić et al. (2017), who reported that the p.Gly380Arg mutation induces conformational changes in the *FGFR3* transmembrane domain that affect downstream signaling [32]. Additionally, the work of Krejci et al. (2012) demonstrated that *FGFR3* mutations alter ligand-binding affinities and receptor trafficking, which may contribute to the variable clinical phenotypes observed in skeletal dysplasias [33]. The comparative docking results indicated comparable binding affinities between wild-type and mutant *FGFR3*, with the wild-type showing a slightly better docking score (-5.5102) compared to the mutant (-4.7056). However, the mutant demonstrated improved placement energy (E_place: -72.6459 vs -53.8522) and refinement energy (E_refine: -22.9815 vs -21.8117), suggesting that while the overall binding affinity is reduced, the mutant may undergo more favorable energetic stabilization during complex formation. These observations align with the computational study by Dabir et al. (2020), who performed molecular docking of *FGFR3* inhibitors and noted that pathogenic mutations can paradoxically enhance certain energy parameters while reducing overall binding scores [29]. The stronger hydrogen bond interaction observed in the wild-type (Arg714: -5.8 kcal/mol) compared to the mutant (Arg172: -2.3 kcal/mol) indicates that the wild-type protein maintains more robust specific interactions with the ligand, which may be compromised in the mutant due to conformational rearrangements. The binding and catalytic sites identified in our study, including the ATP-binding region (residues 478-486) and the catalytic residue D617, are consistent with the functional annotation provided by UniProtKB and PROSITE-ProRule. These sites are critical for the kinase activity of *FGFR3*, and their disruption has been implicated in the pathogenesis of skeletal dysplasias, as reviewed by Lievens et

al., (2003) [30]. Chen et al. (2018) further emphasized that mutations affecting the kinase domain or its regulatory regions can lead to gain-of-function or loss-of-function phenotypes depending on the specific residue altered and the cellular context [31].

This study reinforces the critical role of *FGFR3* in regulating endochondral ossification and skeletal development. The identification and characterization of the c.1138G>A (p.Gly380Arg) variant in the Pakistani population, as previously reported by Muhammad et al. (2021), highlights the importance of population-specific genetic screening for achondroplasia and other skeletal dysplasias [14]. Integrating bioinformatics, in silico analyses, and structural modeling provides a powerful approach to elucidate the molecular mechanisms underlying *FGFR3*-related disorders. These findings not only expand the understanding of *FGFR3* mutation effects but also offer valuable insights into genetic counseling, early diagnosis, and future therapeutic strategies, including the development of *FGFR3*-specific inhibitors currently under investigation for the treatment of achondroplasia, as discussed by Hoover-Fong et al. (2020) and Savarirayan et al. (2019) [32, 33].

Conclusion

This study successfully characterized the *FGFR3* c.1138G>A (p.Gly380Arg) variant, confirming it as the primary genetic cause of achondroplasia. Population frequency analysis using gnomAD v4.1.1 revealed a global allele frequency of 0.000004339, with the highest prevalence in European populations. Pathogenicity predictions classified the variant as deleterious, with the substitution of glycine by arginine at position 380 disrupting the transmembrane domain, leading to constitutive receptor activation and impaired chondrocyte proliferation in the growth plate. Protein-protein interaction network analysis confirmed that *FGFR3* interacts with other FGFR family members and heparan sulfate proteoglycans (HSPG2, SDC1, SDC4), which serve as essential co-receptors for FGF signaling. Molecular docking revealed that the wild-type protein exhibited a higher docking score (-5.5102) and stronger hydrogen bond interactions with Gly712 and Arg714 compared to the mutant (-4.7056), which interacted with Ser129 and Arg172. This shift in binding residues suggests that the mutation alters the conformational landscape of the binding pocket. Clinically, these findings support targeted genetic screening for achondroplasia in different populations and provide structural insights that may inform future therapeutic strategies, including *FGFR3*-specific inhibitors.

References

1. Krakow D, Rimoin DL. The skeletal dysplasias. *Genet Med*. 2010;12(6):327-341.
2. Mortier GR, Cohn DH, Cormier-Daire V, et al. Nosology and classification of genetic skeletal disorders: 2019 revision. *Am J Med Genet A*. 2019;179(12):2393-2419.
3. Horton WA, Hall JG, Hecht JT. Achondroplasia. *Lancet*. 2007;370(9582):162-172.
4. Bonafe L, Cormier-Daire V, Hall C, et al. Nosology and classification of genetic skeletal disorders: 2015 revision. *Am J Med Genet A*. 2015;167A(12):2869-2892.
5. Unger S, Ferreira CR, Mortier GR, et al. Nosology of genetic skeletal disorders: 2023 revision. *Am J Med Genet A*. 2023;191(5):1164-1209.
6. Stals KL, Wakeling M, Baptista J, et al. Diagnosis of lethal or prenatal-onset autosomal recessive disorders by whole exome sequencing. *Prenat Diagn*. 2018;38(1):33-43.
7. Muhammad N, Yasin S, Fatima Z, ul Ain N, Faizan M, Naz S. The c.1138G>A Variant of Fibroblast Growth Factor Receptor 3 is a Common Cause of Achondroplasia in Pakistan. *Pak J Zool*. 2021;53(6):2519-2521.
8. Piñero J, Ramírez-Anguita JM, Saüch-Pitarch J, et al. The DisGeNET knowledge platform for disease genomics: 2019 update. *Nucleic Acids Res*. 2020;48(D1):D845-D855.
9. Rappaport N, Twik M, Plaschkes I, et al. MalaCards: an amalgamated human disease compendium with diverse clinical and genetic annotation and structured search. *Nucleic Acids Res*. 2017;45(D1):D877-D887.
10. Oliveros JC. Venny. An interactive tool for comparing lists with Venn diagrams. 2007-2015.
11. Amberger JS, Bocchini CA, Scott AF, Hamosh A. OMIM.org: leveraging knowledge across phenotype-gene relationships. *Nucleic Acids Res*. 2019;47(D1):D1038-D1043.

12. Schwarz JM, Cooper DN, Schuelke M, Seelow D. MutationTaster2: mutation prediction for the deep-sequencing age. *Nat Methods*. 2014;11(4):361-362.
13. Rentzsch P, Witten D, Cooper GM, Shendure J, Kircher M. CADD: predicting the deleteriousness of variants throughout the human genome. *Nucleic Acids Res*. 2019;47(D1):D886-D894.
14. Pettersen EF, Goddard TD, Huang CC, et al. UCSF Chimera—a visualization system for exploratory research and analysis. *J Comput Chem*. 2004;25(13):1605-1612.
15. Waterhouse A, Bertoni M, Bienert S, et al. SWISS-MODEL: homology modelling of protein structures and complexes. *Nucleic Acids Res*. 2018;46(W1):W296-W303.
16. Kim S, Chen J, Cheng T, et al. PubChem 2023 update. *Nucleic Acids Res*. 2023;51(D1):D1373-D1380.
17. Trott O, Olson AJ. AutoDock Vina: improving the speed and accuracy of docking with a new scoring function, efficient optimization, and multithreading. *J Comput Chem*. 2010;31(2):455-461.
18. Shiang R, Thompson LM, Zhu YZ, et al. Mutations in the transmembrane domain of *FGFR3* cause the most common genetic form of dwarfism, achondroplasia. *Cell*. 1994;78(2):335-342.
19. Bellus GA, Hefferon TW, Ortiz de Luna RI, et al. Achondroplasia is defined by recurrent G380R mutations of *FGFR3*. *Am J Hum Genet*. 1995;56(2):368-373.
20. Willet K, Dunn A, Brown M, et al. Population-specific frequencies of *FGFR3* mutations in global genomic databases. *Eur J Hum Genet*. 2023;31(4):456-463.
21. Vajo Z, Francomano CA, Wilkin DJ. The molecular and genetic basis of fibroblast growth factor receptor 3 disorders: the achondroplasia family of skeletal dysplasias, Muenke craniosynostosis, and Crouzon syndrome with acanthosis nigricans. *Endocr Rev*. 2000;21(1):23-39.
22. Ornitz DM, Itoh N. The Fibroblast Growth Factor signaling pathway. *Wiley Interdiscip Rev Dev Biol*. 2015;4(3):215-266.
23. Eswarakumar VP, Lax I, Schlessinger J. Cellular signaling by fibroblast growth factor receptors. *Cytokine Growth Factor Rev*. 2005;16(2):139-149.
24. Murakami M, Elfenbein A, Simons M. Non-canonical fibroblast growth factor signalling in angiogenesis. *Cardiovasc Res*. 2008;78(2):223-231.
25. Webster MK, Donoghue DJ. Constitutive activation of fibroblast growth factor receptor 3 by the transmembrane domain point mutation found in achondroplasia. *EMBO J*. 1996;15(3):520-527.
26. Tavormina PL, Shiang R, Thompson LM, et al. Thanatophoric dysplasia (types I and II) caused by distinct mutations in fibroblast growth factor receptor 3. *Nat Genet*. 1995;9(3):321-328.
27. Tomić S, Hönigschmid P, Schmid F, et al. Molecular dynamics simulations of *FGFR3* transmembrane domain mutations in skeletal dysplasias. *J Biomol Struct Dyn*. 2017;35(8):1723-1735.
28. Krejci P, Masri B, Salazar V, et al. Bisindolylmaleimide I suppresses fibroblast growth factor receptor 3 dimerization and prevents ERK activation in achondroplasia. *Arthritis Res Ther*. 2012;14(4):R170.
29. Dabir P, Kashyap M, Rathi B, et al. In silico docking and molecular dynamics simulation of *FGFR3* inhibitors in achondroplasia. *J Mol Graph Model*. 2020;101:107755.
30. Lievens PM, Liboi E. The thanatophoric dysplasia type II mutation hampers complete maturation of fibroblast growth factor receptor 3 (*FGFR3*), which activates signal transducer and activator of transcription 1 (STAT1) from the endoplasmic reticulum. *J Biol Chem*. 2003;278(19):17344-17349.
31. Chen L, Yang Y, Yang C, et al. *FGFR3* mutation analysis in Chinese patients with achondroplasia. *Mol Genet Genomic Med*. 2018;6(6):1103-1110.
32. Hoover-Fong JE, Alade AY, Ain MC, et al. Achondroplasia: natural history and management. *Am J Med Genet C Semin Med Genet*. 2020;184(4):1029-1041.
33. Savarirayan R, Irving M, Bacino CA, et al. C-type natriuretic peptide analogue therapy in children with achondroplasia. *N Engl J Med*. 2019;381(1):25-35.